



Clouds, regional surface albedo and the

Petri

Finnish Meteorological Institute, Climate Change

1. Introduction

In the presence of clouds, the downwelling solar irradiance at the surface F^{\downarrow} can be enhanced greatly by multiple reflections between a high-albedo surface and the cloud layer. However, F^{\downarrow} depends not only on the local surface albedo but on the distribution of albedo up to tens of kilometres away from the observation site (Fig. 1). This complicates the interpretation of solar irradiance measurements (e.g.) at typical near-costal Arctic or Antarctic observation sites with a large contrast between snow and ocean surface albedos.

Pirazzini and Räisänen (JGR 2008; hereafter PR08) studied the influence of a heterogeneous surface on F^{\downarrow} using a backward Monte Carlo radiative transfer model. A parameterization was derived for the broadband **effective surface albedo** α_{eff} of a heterogeneous surface, defined as the albedo of a homogeneous surface that would result in the same downwelling irradiance as measured at the observation point in the presence of a heterogeneous surface.

In the present study, **we extend the work of PR08 by considering spectral variations across the solar spectrum.**



Fig. 1. The nature of the problem (photo by Roberta Pirazzini, FMI).

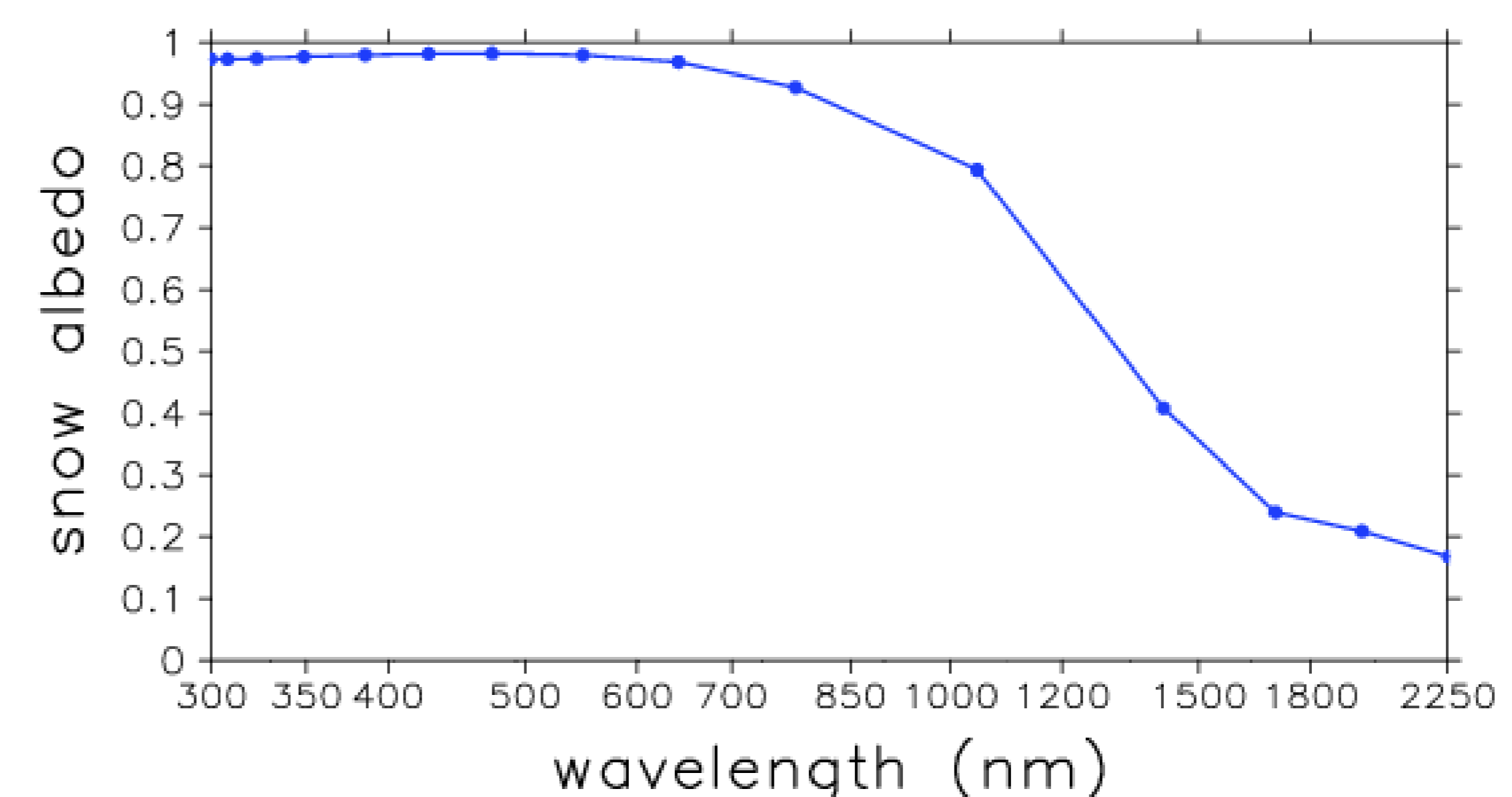


Fig. 2. Assumed spectral albedo of snow (based on measurements in Antarctica; Grenfell et al. 1994).

2. Radiative transfer calculations

A backward 3-D Monte Carlo model is used for radiative transfer calculations. The model **keeps track of the statistics of surface reflections**. These statistics are of interest for parameterizing the effective albedo of a heterogeneous surface.

- $f(r)$ = probability that a photon coming to the observation site has experienced a surface reflection at a distance r
- $p(r)$ = corresponding normalized probability: $p(r) = f(r) / \int_0^{\infty} f(r) dr$
- $P(r)$ = cumulative normalized probability: $P(r) = \int_0^{\infty} p(r') dr'$

The Monte Carlo model is combined with the Ramaswamy and Freidenreich (JGR 1999) scheme for gaseous absorption and Rayleigh scattering. Atmospheric and surface properties are specified as follows:

- a horizontally homogeneous cloud layer embedded in an Arctic summer atmospheric profile
- a Lambertian surface. For snow, Grenfell et al. (JGR 1994) spectral albedo is used (Fig. 2). Ocean albedo is set to 0.1.
- a solar zenith angle of 60 degrees

downwelling solar irradiance: spectral dependence

Räisänen

Research Unit, Helsinki, Finland (petri.raisanen@fmi.fi)

3. Distribution of surface reflections: a homogeneous snow surface

Figure 3 shows $f(r)$, $p(r)$ and $P(r)$ for four spectral bands and three cloud base heights ($z_b=0.2$ km, 1.0 km and 3 km), for a fixed cloud optical depth $\tau=10$.

- The number of surface reflections $f(r)$ decreases with increasing wavelength, mainly because of the reduction in snow albedo.
- For $p(r)$ and $P(r)$, cloud base height plays the dominant role: the higher the cloud base, the larger region influences F^\downarrow at the observation site.
- The relative role of far-away surface reflections generally decreases with increasing wavelength; i.e., for a given distance r , the values of $P(r)$ are larger. Physical reasons: spectral variation of snow albedo, Rayleigh scattering, cloud droplet and water vapour absorption.

Figure 4 further illustrates the cumulative normalized probability $P(r)$. In the UVA region, a pronounced "bulge" towards larger distances appears in the higher percentiles of $P(r)$, especially for optically thin low clouds ($\tau=2.5$, $z_b=0.2$ km). This results from Rayleigh scattering above the cloud, which makes the observed F^\downarrow to feel the impact of surprisingly far-away surface reflections.

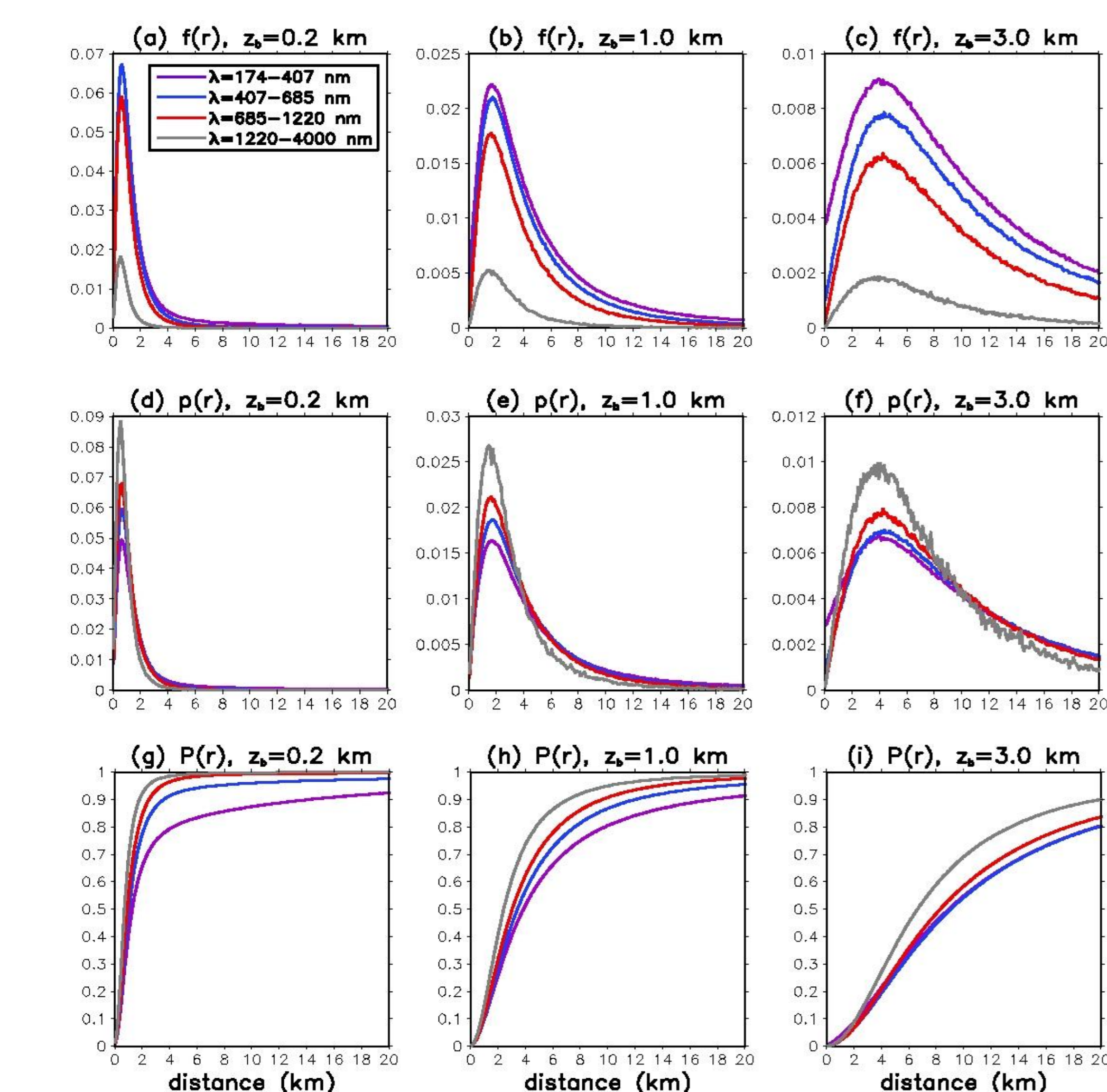


Fig. 3. Statistics of surface reflections contributing to the downwelling solar irradiance F^\downarrow at the observation site, for a homogeneous snow surface and cloud optical depth $\tau=10$. (a)-(c): $f(r)$ = number of reflections per a distance bin of $\Delta r=100$ m; (d-f) normalized probability $p(r)$, and (g-i) cumulative normalized probability $P(r)$.

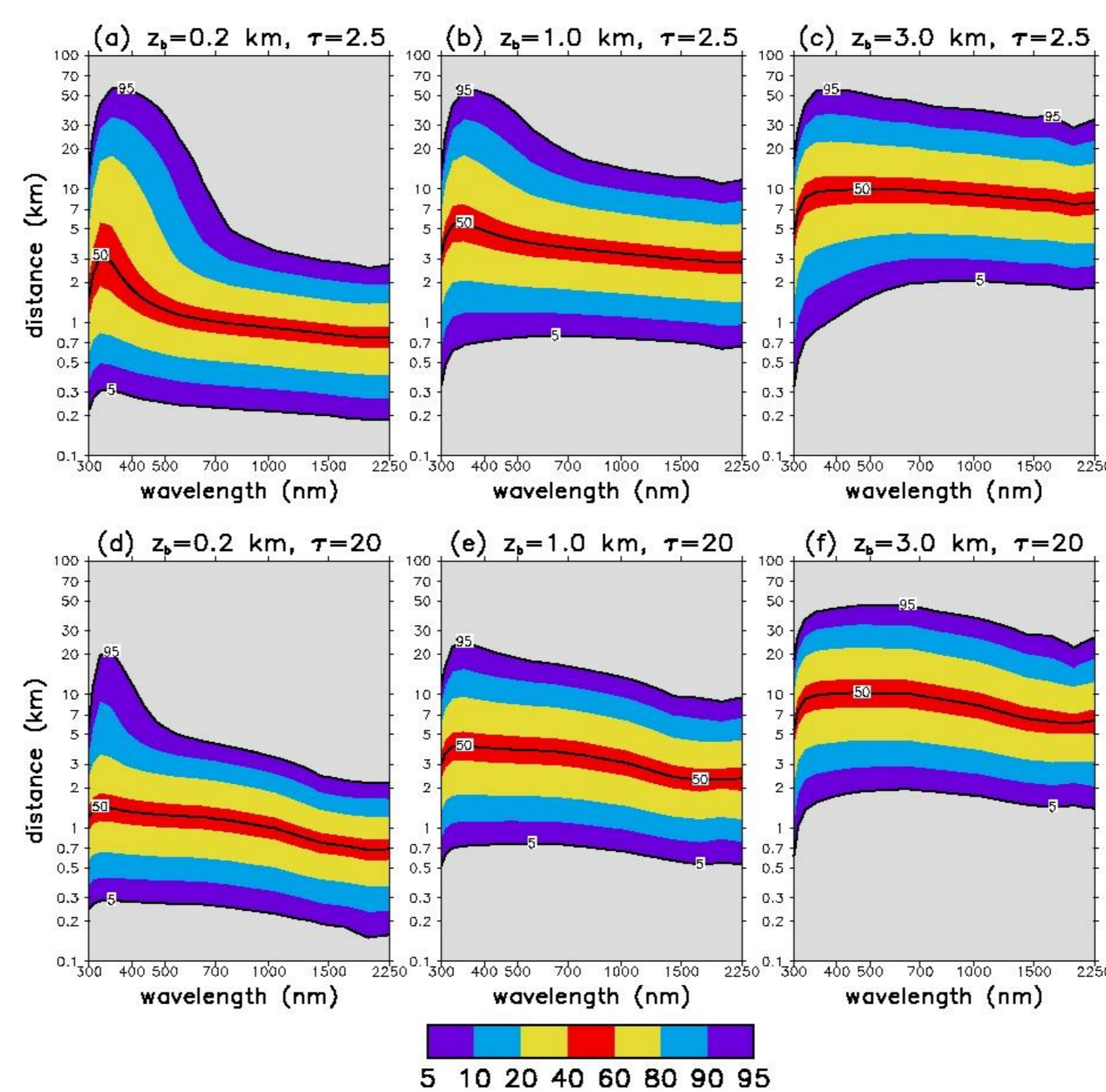


Fig. 4. Cumulative normalized probability of surface reflections $P(r)$ [%] vs. wavelength λ [nm], for a homogeneous snow surface and cloud optical depths of (a)-(c) $\tau=2.5$ and (d)-(f) $\tau=20$. Interpretation: e.g. for $\lambda=350$ nm, $z_b=0.2$ km and $\tau=2.5$, 5% of the surface reflections contributing to the measured F^\downarrow occur closer than 300 m of the observation site, and 5% further than 55 km.

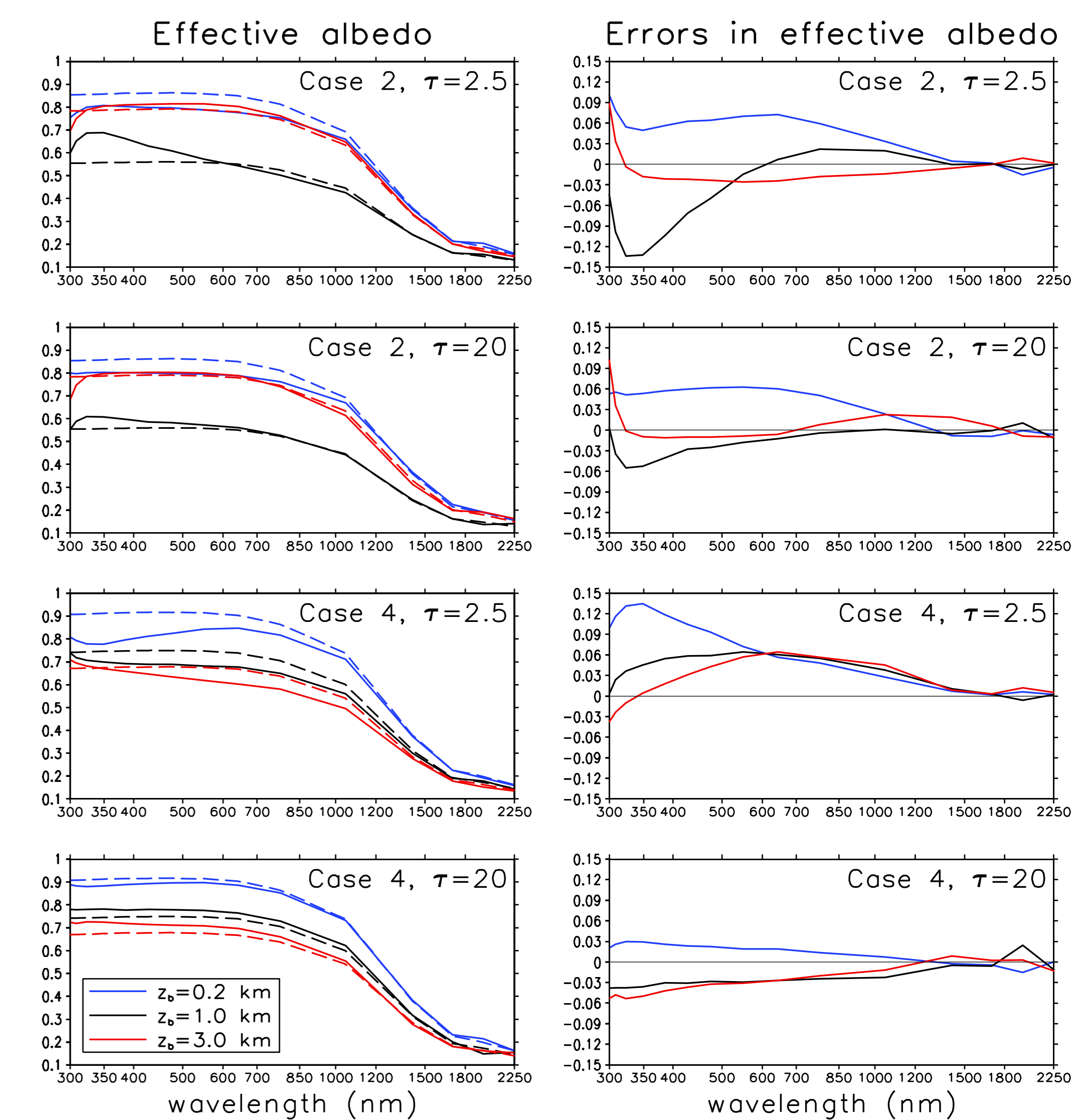


Fig. 5: (left) Effective surface albedo for two surface albedo patterns (Cases 2 and 4 in PR 08), two cloud optical depths ($\tau=2.5$ and $\tau=20$) and three cloud base heights ($z_b=0.2$ km, 1.0 km and 3.0 km). Solid line = Monte Carlo results; dashed line = parameterization by PR08. (right) Errors for the parameterization. The corresponding surface patterns are shown in the bottom (cross = observation site, gray = snow, black = ocean).

4. Spectral effective albedo α_{eff} of a heterogeneous surface

Figure 5 shows spectral α_{eff} as a function of cloud base height ($z_b=0.2$ km, 1.0 km and 3 km) and cloud optical depth ($\tau=2.5$ and $\tau=20$), for two surface albedo patterns (Cases 2 and 4 in PR 08).

- The values of α_{eff} depend strongly on wavelength, decreasing in the near-IR due to low snow albedo.
- There is also a large (and in Case 2, non-monotonic) dependence on cloud base height.
- The parameterization of PR08 captures fairly well the actual dependence of α_{eff} on cloud base height and spectral band. Largest errors (up to 0.13) occur in the UVA region for optically thin clouds. They are related to the effect of Rayleigh scattering occurring above the cloud.